

Enhancing of catalytic properties of vanadia via surface doping with phosphorus using atomic layer deposition

Cite as: J. Vac. Sci. Technol. A **34**, 01A135 (2016); <https://doi.org/10.1116/1.4936390>

Submitted: 27 August 2015 . Accepted: 12 November 2015 . Published Online: 11 December 2015

Verena E. Stempel, Daniel Löffler, Jutta Kröhnert, Katarzyna Skorupska, Benjamin Johnson, Raoul Naumann d'Alnoncourt, Matthias Driess, and Frank Rosowski



View Online



Export Citation



CrossMark

ARTICLES YOU MAY BE INTERESTED IN

[Atomic layer deposition on porous powders with in situ gravimetric monitoring in a modular fixed bed reactor setup](#)

Review of Scientific Instruments **88**, 074102 (2017); <https://doi.org/10.1063/1.4992023>

[Surface chemistry of atomic layer deposition: A case study for the trimethylaluminum/water process](#)

Journal of Applied Physics **97**, 121301 (2005); <https://doi.org/10.1063/1.1940727>

[Review Article: Catalysts design and synthesis via selective atomic layer deposition](#)

Journal of Vacuum Science & Technology A **36**, 010801 (2018); <https://doi.org/10.1116/1.5000587>

AVS Quantum Science

Co-Published by



RECEIVE THE LATEST UPDATES



Enhancing of catalytic properties of vanadia via surface doping with phosphorus using atomic layer deposition

Verena E. Stempel

BasCat - UniCat BASF JointLab, Technische Universität Berlin, Sekr. EW K 01, Hardenbergstraße 36, 10623 Berlin, Germany

Daniel Löffler

Process Research and Chemical Engineering, BASF SE, Carl-Bosch-Straße 38, 67056 Ludwigshafen, Germany

Jutta Kröhnert, Katarzyna Skorupska, and Benjamin Johnson

Department of Inorganic Chemistry, Fritz-Haber-Institut der Max-Planck-Gesellschaft, Faradayweg 4-6, 14195 Berlin, Germany

Raoul Naumann d'Alnoncourt^{a)}

BasCat - UniCat BASF JointLab, Technische Universität Berlin, Sekr. EW K 01, Hardenbergstraße 36, 10623 Berlin, Germany

Matthias Driess

BasCat - UniCat BASF JointLab, Technische Universität Berlin, Sekr. EW K 01, Hardenbergstraße 36, 10623 Berlin, Germany and Technische Universität Berlin, Institut für Chemie, Sekr. C2, Straße des 17. Juni 135, 10623 Berlin, Germany

Frank Rosowski

BasCat - UniCat BASF JointLab, Technische Universität Berlin, Sekr. EW K 01, Hardenbergstraße 36, 10623 Berlin, Germany and Process Research and Chemical Engineering, BASF SE, Carl-Bosch-Straße 38, 67056 Ludwigshafen, Germany

(Received 27 August 2015; accepted 12 November 2015; published 11 December 2015)

Atomic layer deposition is mainly used to deposit thin films on flat substrates. Here, the authors deposit a submonolayer of phosphorus on V_2O_5 in the form of catalyst powder. The goal is to prepare a model catalyst related to the vanadyl pyrophosphate catalyst $(VO)_2P_2O_7$ industrially used for the oxidation of *n*-butane to maleic anhydride. The oxidation state of vanadium in vanadyl pyrophosphate is 4+. In literature, it was shown that the surface of vanadyl pyrophosphate contains V^{5+} and is enriched in phosphorus under reaction conditions. On account of this, V_2O_5 with the oxidation state of 5+ for vanadium partially covered with phosphorus can be regarded as a suitable model catalyst. The catalytic performance of the model catalyst prepared via atomic layer deposition was measured and compared to the performance of catalysts prepared via incipient wetness impregnation and the original V_2O_5 substrate. It could be clearly shown that the dedicated deposition of phosphorus by atomic layer deposition enhances the catalytic performance of V_2O_5 by suppression of total oxidation reactions, thereby increasing the selectivity to maleic anhydride.

© 2015 American Vacuum Society. [<http://dx.doi.org/10.1116/1.4936390>]

I. INTRODUCTION

Selective oxidation reactions are of great interest for the (petro-)chemical industry, especially concerning the upcoming raw material change. However, the direct oxidation of alkanes, e.g., from natural gas, to produce bulk and platform chemicals is not yet conventional. Industry lacks sufficient active and selective catalysts. The only successfully established reaction is the selective oxidation of *n*-butane to maleic anhydride (MAN) with vanadyl pyrophosphate $(VO)_2P_2O_7$ (VPP) catalyst.^{1–7} MAN is produced in a megaton per year range with a yield around 60%. The understanding of the mode of operation of VPP is of general interest to improve and reasonably design selective alkane oxidation

catalysts. However, the reaction mechanism has not been identified until now.^{8,11} VPP and its precursors are extremely dynamic and can form several metastable phases under oxidation conditions with *n*-butane.^{10–14} Hence, the resulting surface differs substantially from a theoretical VPP single crystal surface. The specific functions of the different surface species in the oxidation process remain mostly unknown. Suggestions have been made, including particular roles for vanadium(IV)–vanadium(V) redox couples, isolated V^{5+} sites, or P–OH Brønsted acidic sites.^{3,9–11} Near-ambient pressure x-ray photoelectron spectroscopy (XPS) measurements showed that the surface features a significant amount of V^{5+} under reaction conditions.^{12–14} The average surface vanadium oxidation state under reaction conditions (400 °C in *n*-butane/ O_2 / H_2O / N_2) is with +4.3 significantly higher than in the bulk (+4.0) and that the surface V/P/O ratio is with 1/1.5/6 different than the bulk ratio of 1/1/4.5.

^{a)}Electronic mail: r.naumann@bascat.tu-berlin.de

Based on the literature results, we propose that V_2O_5 doped at its surface with phosphorus can be a highly simplified model for the VPP catalyst. To test our hypothesis, we prepared several catalysts consisting of V_2O_5 partially covered with phosphorus at the surface. We used equipment and techniques usually applied for atomic layer deposition for the surface doping of the V_2O_5 with phosphorus. Our aim is not to create thin layers of phosphorus oxide on V_2O_5 but only to cover the surface of V_2O_5 partially with phosphorus. Thus, it can be debated whether our experiments can be called atomic layer deposition (ALD) experiments in common. As we plan to do this partial coverage in a single ALD cycle, the usually reported tests to prove the successful application of ALD (growth per cycle diagrams, etc.) cannot be shown in our case. However, the conditions used for the deposition of phosphorus on V_2O_5 were successfully applied for deposition of $AlPO_4$ layers on silicon wafers.

ALD is traditionally a thin film deposition technique, which uses usually two vapor phase precursors.^{15,16} A substrate is sequentially exposed to an overdose of the precursors. The precursor molecules react with the surface OH groups until saturation. ALD is always self-limiting, as the reaction terminates once all the reactive sites on the surface are consumed. ALD is mainly applied to deposit thin films on flat substrates such as silicon wafers, e.g., for electronic materials. In literature, it was shown that ALD can also be a promising new technique for the synthesis of catalytic materials, including substrates in the form of powder.^{17,18} The self-limiting character of the reactions makes it possible to achieve uniformly distributed deposits on porous high-surface-area solids, which are of particular interest for catalysis. Unlike other traditional catalyst synthesis routes (e.g., impregnation, grafting), ALD largely preserves the original surface structure. The support is not moistened or brought in contact with other solvents during ALD.

For comparison, phosphorus was also deposited on the surface of V_2O_5 via incipient wetness impregnation. Incipient wetness impregnation (IWI) is a traditional synthesis route for heterogeneous catalysts. Usually, an active metal precursor is dissolved in an aqueous or organic solution. Then, a volume of the metal-containing solution equaling the free pore volume of the substrate is added to the substrate filling the pores completely. The impregnated substrate is then dried and calcined to remove all volatile components of the added solution, depositing the metal on the catalyst surface. In our case, we use phosphorus instead of a metal, water as solvent, and the V_2O_5 as substrate.

Finally, all prepared catalysts and the original V_2O_5 as reference were catalytically tested for the oxidation of *n*-butane to maleic anhydride under standard conditions comparable to the industrial process.

II. EXPERIMENT

A. Chemicals

Vanadium(V) oxide (V_2O_5 , min. 99.9%, high-purity, GfE) was pressed without binder at ~ 185 MPa, crushed, and sieved to a particle size fraction of 100–200 μm . The oxide

was preheated to 393 K in constant air flow (500 ml/min) to remove the adsorbed water prior to ALD or impregnation experiments. Trimethylaluminum ($[\text{CH}_3]_3\text{Al}$ TMA, electronic grade, $\geq 99.9999\%$, Aldrich), oxalic acid ($\text{C}_2\text{H}_2\text{O}_4$, puriss. p.a., $\geq 99.0\%$, Sigma-Aldrich), water (H_2O , CHROMASOLV, for HPLC, Sigma-Aldrich), phosphoric acid (H_3PO_4 , 85 wt. % in H_2O , 99.99%, trace metals basis, Aldrich), and P-ICP standard (TraceCERT, Fluka) were used without further purification. The ALD precursor tris(dimethylamino)phosphine ($[\text{Me}_2\text{N}]_3\text{P}$, HMPT, 97%, Aldrich) was fractionally distilled under N_2 twice.

B. Catalyst synthesis

1. Atomic layer deposition

The ALD experiments were conducted in a Beneq TFS 200 cross-flow system (Beneq Oy, Espoo, Finland). Prior to the experiments depositing P on V_2O_5 , suitable process parameters for the HMPT precursor were established. HMPT was deposited together with TMA as AlPO_4 on silicon wafers (diameter of 200 mm). H_2O served as the oxygen source and pure N_2 gas (99.999%) served as carrier and purge gas. The different precursors were alternately pulsed into the reaction chamber. One ALD cycle consisted of eight steps and followed a dose-purge sequence of $(\text{Me}_2\text{N})_3\text{P}$ (0.1 s)– N_2 (3 s)– H_2O (0.1 s)– N_2 (3 s)–TMA (3.5 s)– N_2 (4 s)– H_2O (0.1 s)– N_2 (3 s). H_2O and TMA were dosed via saturators at 25 °C. The saturator for HMPT was heated to 30 °C. During deposition, the reaction chamber was maintained at 1.0 mbar and 120 °C with a steady flow of N_2 of 300 ml/min. The thickness of the deposited film was analyzed with a SENTECH multiple angle laser ellipsometer SE 400adv in mapping mode.

The catalyst sample ALD-P/ V_2O_5 was prepared with a silicon wafer as a sample holder for the V_2O_5 powder. Five grams of the oxide were uniformly spread over the wafer to give a height of the powder layer below 2 mm. As above, the saturator temperature was 30 °C, the substrate temperature was 120 °C, and the pressure in the reaction chamber was 1.0 mbar in a flow of 300 ml/min of N_2 . One single ALD cycle was performed on 5 g V_2O_5 with three pulses of $(\text{Me}_2\text{N})_3\text{P}$ (each 3.5 s), N_2 purge (300 s), 500 O_3 pulses (each 2.5 s), and a final N_2 purge (300 s). O_3 was generated with the built-in ozone generator HyXo BMT 803N (HyXo Oy, Kerava, Finland) using pure oxygen (99.999%) as feed gas. O_3 production was 8 g/h (at 100 g/Nm³ at 20 °C).

2. Incipient wetness impregnation

A sample series of P/ V_2O_5 was prepared using IWI.^{19,20} H_3PO_4 or HMPT served as precursors and their desired amounts were diluted in water. The total volume of solution corresponded to the pore volume of V_2O_5 (0.72 ml/g), which was determined in advance. The oxide was impregnated with the precursor solution and dried in constant flow of air (500 ml/min) for 2 h at 110 °C. The powders were subsequently calcined under continuous air flow (500 ml/min) at 450 °C for 5 h.

C. Characterization

N₂ physisorption measurements were performed at liquid N₂ temperature on a Quantachrome Autosorb-6B analyzer. Prior to the measurement, the samples were outgassed in vacuum at 150 °C for 2 h. The specific surface area S_{BET} was calculated according to the multipoint Brunauer–Emmett–Teller method (BET).

Fourier transform infrared spectra (FTIR) were collected on a Perkin-Elmer PE 100 spectrometer equipped with a deuterated triglycine sulfate pyroelectric detector (64 accumulated scans, 4 cm⁻¹ resolution). The samples were pressed (371 MPa) into infrared transparent, self-supporting wafers (typically 10–16 mg/cm²), which were placed in an *in situ* infrared transmission cell. The IR cell was directly connected to a vacuum system equipped with a gas dosing line. The catalysts were pretreated in vacuum (10⁻⁶ mbar) at 473 K for 1 h. Following this, ammonia was adsorbed at 293 K by increasing the equilibrium pressure to 7 mbar for 90 min. The gas phase was subsequently removed at 353 K (10⁻⁶ mbar for 30 min). The spectra have been taken in ammonia every 30 min and before and after gas desorption at 293 K.

The P content of the samples was determined with an inductively coupled plasma-optical emission spectroscopy (ICP-OES, Varian 720-ES). The powders were dissolved in water using oxalic acid prior to ICP-OES measurements. The spectroscope was five-point calibrated with a commercially available, diluted standard for P.

XPS measurements were performed in a vacuum chamber (10⁻⁸ mbar) using a Phoibos 150 MCD-9 hemispherical analyzer and an Al K α x-ray source (1486.6 eV). The resulting peaks were normalized by number of sweeps, inelastic mean free path, analyzer transmission function, and absorption cross section. The energy scale was calibrated with sputter-cleaned gold (Au 4f_{7/2} = 84.0 eV) and copper (Cu 2p_{3/2} = 932.7 eV).

Powder x-ray diffraction (XRD) measurements were performed on a STOE STADI P transmission diffractometer equipped with a primary focusing Ge monochromator (Cu K α ₁ radiation) and DECTRIS MYTHEN 1K position sensitive solid-state detector. The samples were mounted in the form of small amounts of powder sandwiched between two layers of polyacetate film and fixed with x-ray amorphous grease.

D. Catalytic testing

Catalytic tests for the selective oxidation of butane to maleic anhydride were carried out in a high-throughput setup (hte GmbH, Heidelberg, Germany). The setup consisted of a gas dosing unit, a reactor unit, and an analytics unit. The setup was fully automated in terms of process control, data processing, and management. The gas dosing unit allowed mixing feeds containing N₂, O₂, *n*-butane, Ar (as internal standard), and H₂O. The reaction was conducted at atmospheric pressure. The reactor unit consisted of eight parallel reactors (outer diameter 18 mm and inner diameter 12 mm) for catalyst samples with a maximum bed volume of 1 ml

and one blank reactor filled with inert material. The reactor temperature was individually controlled for each reactor in the range of 250–550 °C. The temperature in the catalyst bed was monitored by a multipoint thermocouple with three measuring points along the fixed bed. The effluent gas of each reactor was analyzed by two gas chromatographs (7890A, Agilent) equipped with thermal conductivity and flame ionization detectors. In addition, the effluent gas of the blank reactor, which equals the inlet gas of all reactors, was analyzed as well. A RTX wax column (Restek) separated oxygenates. A HP-Plot Q column (Agilent) separated alkanes and olefins. Permanent gases were separated using a parallel combination of CP-Molsieve and PoraBOND Q columns (Agilent).

The catalytic test was carried out in a gas mixture of 2% butane, 3% steam, 3% argon, and 20% O₂ balanced with N₂. The gas hourly space velocity (GHSV) was fixed to 2000 h⁻¹. The catalyst beds consisted of 1 ml of a sieve fraction of 100–200 μm , respectively. The catalyst performance was tested in a temperature range starting from 300 to 450 °C in steps of 25 K. Each temperature was held for 12 h. During this time, the effluent gas of each reactor including the blank reactor was analyzed five times. After reaching the final temperature of 450 °C, the temperature steps at 375, 350, and 325 °C were repeated to check for activation or deactivation of the catalyst samples with time on stream.

III. RESULTS AND DISCUSSION

A. V₂O₅ reference characterization

The V₂O₅ starting material was analyzed with FTIR spectroscopy of adsorbed ammonia to determine the concentration of acidic hydroxyl groups at the surface. The spectrum of the preheated V₂O₅ sample in vacuum was taken as a reference. Both, the spectrum obtained in the presence of gas-phase NH₃ and the spectrum recorded after desorption of physisorbed NH₃ are presented in Fig. 1. The adsorbed ammonia on the surface gives mainly three bands.^{21,22} The peak at 1423 cm⁻¹ is attributed to the asymmetric deformation vibration of ammonium ions formed by reaction of NH₃ with Brønsted acid sites. The band of the corresponding symmetric deformation vibration is found as a weak feature near 1670 cm⁻¹. Lewis acid sites on the surface of the oxide are indicated by peaks corresponding to symmetric and asymmetric deformation vibrations of coordinately bonded ammonia molecules at 1300–1150 and 1611 cm⁻¹, respectively.

The concentration of Brønsted acid sites is 9 $\mu\text{mol/g}$, which has been calculated based on the integrated area of the peak at 1423 cm⁻¹ applying an extinction coefficient of $\epsilon = 2.15 \cdot 10^5 \text{ cm}^2/\text{mol}$.^{21,22} The extinction coefficient has been determined in the literature for the asymmetric deformation vibration of ammonium ions adsorbed on Al₂O₃-supported vanadia. A surface area of 3.87 m²/g was calculated based on the adsorption isotherm of nitrogen measured at 77 K and the multipoint BET. Together with the OH site concentration, the OH surface density can be calculated to 2.33 $\mu\text{mol/m}^2$, which corresponds to 1.4 OH sites/nm².

In addition to FTIR, XRD and XPS studies have been conducted with the pure V_2O_5 . The recorded XRD pattern confirms the phase purity of the V_2O_5 (Fig. 3). XPS studies verify the oxidation state of +5 for vanadium (Fig. 2).

B. Phosphorus atomic layer deposition

In preliminary experiments, the phosphorus precursor was deposited on silicon wafers together with TMA and water as an oxygen source yielding $AlPO_4$. A dosing temperature of 30 °C for the P precursor and substrate temperature of 120 °C led to a uniform coating of the entire wafer. The conformity of the wafer coating was confirmed with ellipsometry. An average thickness of 26.2 nm was reached after 200 ALD cycles. This corresponds to an average growth per cycle of 1.31 Å/cycle. The ascertained average refractive index of 1.550 is in good agreement with the literature value of $AlPO_4$ $n_D = 1.546$.²³ There are several literature reports about different ALD processes for the formation of $AlPO_4$. Hämäläinen *et al.* deposited $AlPO_4$ with aluminum chloride $AlCl_3$ and trimethylphosphate $(CH_3O)_3PO$. They obtained a growth rate of 1.4 Å/cycle and a refractive index of 1.5 at a deposition temperature of 150 °C.²⁴ At the same deposition temperature Liu *et al.* reached 1.7 Å/cycle with TMA and trimethylphosphite.²⁵ The reported processes have been proven to be self-limiting due to the linear relationship between film thickness and ALD cycle number. Our results for average growth rate and refractive index are in excellent agreement with the reported ALD experiments. As our experimentation time at the Beneq facility was limited, we did not investigate the deposition of $AlPO_4$ in more detail, e.g., measuring saturation curves or thickness-cycle number plots. We were not primarily interested in the formation of thick layers of $AlPO_4$, but needed to determine suitable temperature parameters for the P precursor. Based on our results,

we assume that our process for deposition of $AlPO_4$ is self-limiting and thus an ALD process.

The temperatures for the formation of $AlPO_4$ were also set for the deposition of P on V_2O_5 using O_3 as oxygen source. The conditions were chosen to ensure full saturation of the V_2O_5 surface with the P precursor in one single ALD cycle. The deposition process was therefore not optimized in time or precursor consumption. Both precursors were highly overdosed. One ALD cycle led to a P/ V_2O_5 ratio of 121.9 µg(P)/g(V_2O_5), which was analyzed with ICP-OES (see Table I). Assuming that one P precursor molecule reacts with one OH site on the surface, we can calculate a surface coverage of 43% based on the OH site density.

Although direct saturation curves for the ALD process were not recorded, e.g., with online mass spectrometry or

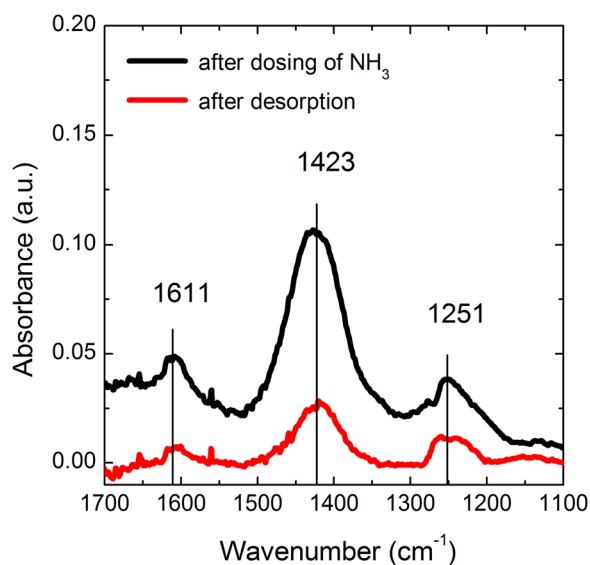


FIG. 1. (Color online) FTIR spectra of ammonia adsorbed on the reference V_2O_5 . The spectra have been taken after NH_3 dosing at 293 K at 7 mbar and desorption of NH_3 in vacuum 10^{-6} mbar at 473 K for 1 h.

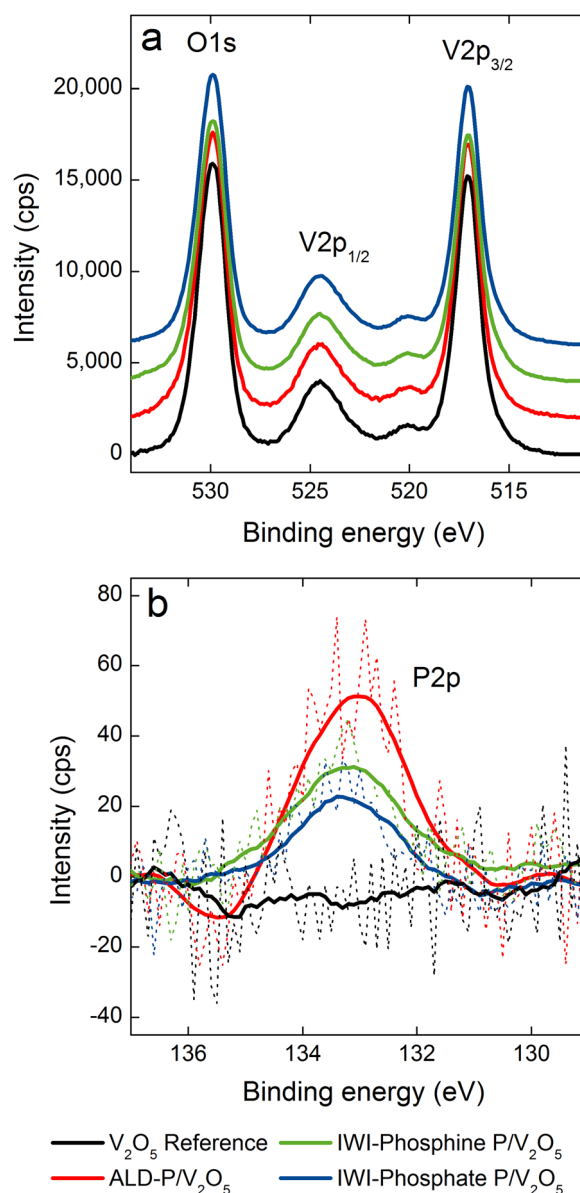


FIG. 2. (Color online) XPS spectra of V_2O_5 reference and P/ V_2O_5 samples: (a) Spectra of the V 2p–O 1s region of vanadium oxide. No peak fitting is shown (plotted with offset for clarity); (b) Spectra of the P 2p (solid lines are included to guide eye).

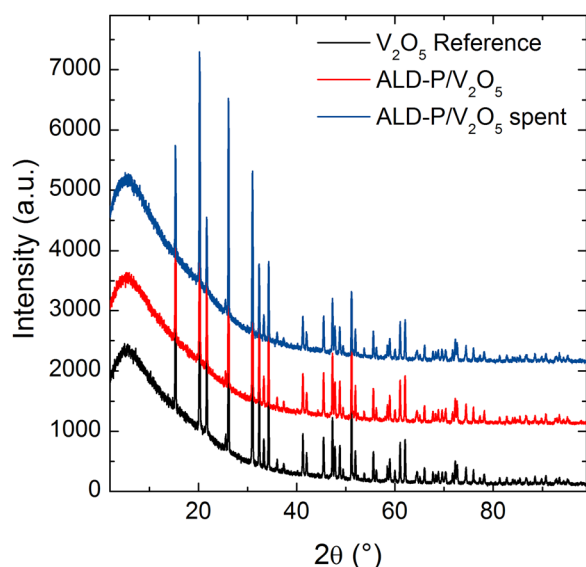


FIG. 3. (Color online) XRD pattern of the starting material V_2O_5 and the ALD-P/ V_2O_5 sample before and after catalytic testing.

quartz crystal microbalance, the low coverage of the V_2O_5 with the precursor strongly indicates a controlled deposition process based on surface saturation.

C. Phosphorus doped V_2O_5 samples characterization

The investigated samples include a V_2O_5 reference sample (99.99%, trace metals basis, Aldrich); an ALD-P/ V_2O_5 sample prepared by ALD [using $(Me_2N)_3P$ and O_3]; an IWI-phosphine P/ V_2O_5 sample [prepared by IWI and $(Me_2N)_3P$ precursor to give the same amount of PO_x as the ALD sample]; an IWI-phosphate P/ V_2O_5 (submonolayer) sample (prepared by IWI and H_3PO_4 precursor to give the same amount of PO_x as the ALD sample) and an IWI-phosphate P/ V_2O_5 (multilayer) sample (prepared by IWI and H_3PO_4 precursors to give a $10\times$ higher amount of PO_x as the ALD sample).

The whole sample family was tested for selective oxidation of *n*-butane. The chemical composition was analyzed with ICP-OES before and after testing. XRD measurements were collected for the reference and the ALD sample before and after testing. XPS measurements were performed for all samples excluding IWI-phosphate P/ V_2O_5 (multilayer).

ICP-OES results are given in Table I. The IWI samples have a lower phosphorus concentration than expected. Considering the boiling points of the P precursors ($162\text{--}164^\circ\text{C}$ for HMPT and 158°C for H_3PO_4), some P might have vaporized during drying and calcination. The P loss can as well be rationalized by a weak surface–precursor interaction after incipient wetness impregnation. Unlike other preparation techniques, e.g., ion exchange or grafting, incipient wetness impregnation is not based on direct chemical reaction between surface and precursor.

Figure 2 shows the V 2p and O 1s XPS region (a) and P 2p region (b) for the three P/ V_2O_5 samples and the reference V_2O_5 . The O 1s and the V 2p peaks superimpose perfectly, showing that the composition of all samples concerning V and O is identical, within the precision of the XPS measurement. The V $2p_{3/2}$ peak maximum is at 517.1 ± 0.1 eV. The O 1s oxygen peak maximum is at 529.9 ± 0.1 eV. The shape as well as the binding energy of the V $2p_{3/2}$ peak is similar to reported values for V_2O_5 and corresponds to a V^{5+} species, as expected for V_2O_5 .²⁶ A very low P 2p peak at 133.3 ± 0.1 eV, indicating a P^{5+} species, appears only for the P/ V_2O_5 samples and confirms the presence of phosphorus after carrying out both synthesis methods, respectively. The peak height correlates with the overall phosphorus concentration in the three low P samples as detected with ICP-OES (see Table I). The P^{+3} precursor $(Me_2N)_3P$ was consequently oxidized up to P^{+5} in both synthesis methods. In ALD, the oxidation agent was O_3 , and during the impregnation, the oxidation probably took place during the calcination in air. The phosphate precursor, which was exclusively impregnated, already had the oxidation state of $+5$ for phosphorus.

The XRD patterns of the V_2O_5 reference material and the ALD-P/ V_2O_5 sample before and after catalytic testing are shown in Fig. 3. All reflections match V_2O_5 crystalline patterns that have been reported before.²⁷ Consequently, the deposition of phosphorus on the surface did not form any new crystalline adphases like vanadyl pyrophosphate or changed the crystallinity of the V_2O_5 itself.

D. Selective oxidation of *n*-butane

The catalytic properties of all four P/ V_2O_5 samples with pure V_2O_5 as reference have been tested for the selective oxidation of *n*-butane to maleic anhydride. Figure 4

TABLE I. Chemical composition of different P/ V_2O_5 samples synthesized with ALD and IWI.

Sample	Sample number ^a	Amount of P $\mu\text{g(P)}/\text{g}(V_2O_5)$		Surface coverage of OH sites by PO_x	
		Before calcination ^b	After calcination/preparation ^c	Fresh catalyst (%) ^d	Spent catalyst (%) ^d
ALD-P/ V_2O_5	0030	—	121.9	43	43
IWI-phosphine P/ V_2O_5	0411	122	81.7	29	26
IWI-phosphate P/ V_2O_5 (submonolayer)	0412	122	66.5	24	20
IWI-phosphate P/ V_2O_5 (multilayer)	0410	1220	1140.0	408	355

^aInternal sample number.

^bThe phosphorus amount before calcination is calculated from the total amount of precursor and V_2O_5 used during preparation of the incipient wet catalyst samples.

^cThe phosphorus content has been analyzed by inductively plasma coupled optical emission spectroscopy (ICP-OES).

^dThe surface coverage is calculated by the P concentration (via ICP-OES) in relation to the OH site concentration.

summarizes the *n*-butane conversion and the selectivity to maleic anhydride at different temperatures for each sample, respectively. The undesired total and partial oxidation by-products are mainly carbon dioxide and carbon monoxide, with a smaller amount of acetic acid (not shown). The time on stream for one temperature step was 12 h, so the samples were 120 h on stream in total.

The original V_2O_5 is mainly a total oxidation catalyst and shows conversions of *n*-butane up to 42.5% at 450 °C. The selectivity to MAN is always below 5%. No MAN at all is detected at temperatures above 375 °C. This can be rationalized by the fact that V_2O_5 is mainly a total oxidation catalyst, and thus any MAN formed combusts to CO_x in consecutive reactions at higher temperatures. However, the results show clearly that V_2O_5 without P can produce MAN with low selectivities. After reaching the highest temperature of 450 °C, the catalyst is slightly less active but more selective. This can be seen by comparing the performance of the catalyst at the temperatures of 375, 350, and 325 °C before and after testing at 450 °C. This effect might be due to

sintering and annealing at higher temperatures, presuming that defect sites are mainly unselective sites for total oxidation.

In comparison, the ALD-P/ V_2O_5 shows lower conversions of butane and higher selectivities to MAN at all temperatures. The general trends observed for V_2O_5 can still be found. ALD-P/ V_2O_5 is also mainly a total oxidation catalyst, burning formed MAN at higher temperatures. But the selectivities to MAN are more than doubled up to temperatures of 375 °C, and MAN is still found at temperatures up to 450 °C. A comparison of catalytic activity at the same temperature levels before and after reaching the maximum temperature of 450 °C indicates a slight deactivation of ALD-P/ V_2O_5 with time on stream. This deactivation cannot be related to phase changes, which are excluded by XRD, or loss of phosphorus, which is excluded by ICP-OES carried out before and after catalytic testing, respectively. Again, the deactivation might be due to sintering and annealing at higher temperatures. The results indicate that phosphorus deposited on the surface of V_2O_5 moderates the activity of V^{5+} sites for

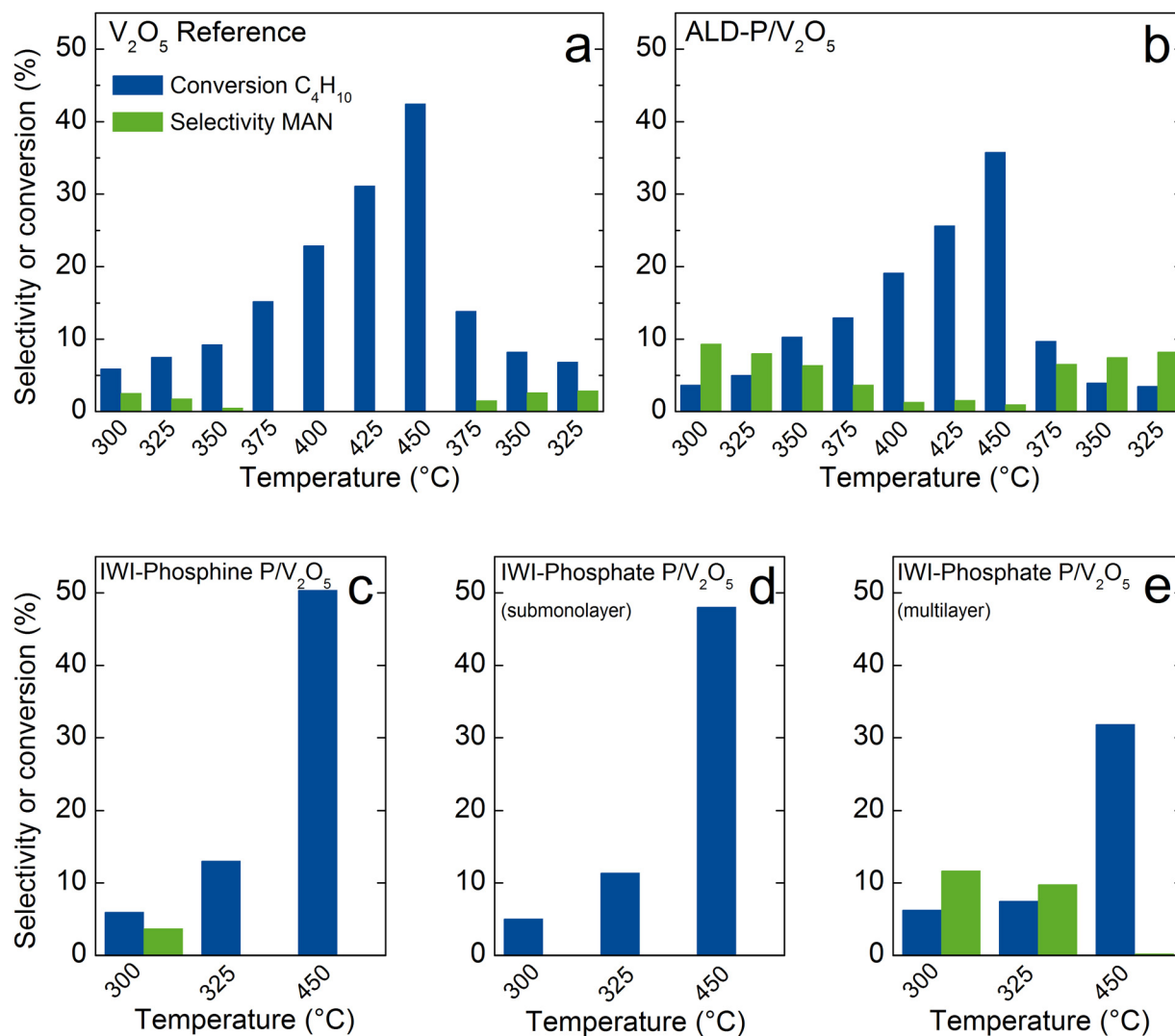


FIG. 4. (Color online) Conversion of *n*-butane (C_4H_{10}) and selectivity to MAN for V_2O_5 reference (a) and P/ V_2O_5 samples [(b)–(e), see description] in the temperature range 300–450 °C with a feed of $C_4H_{10}/O_2/H_2O/Ar/N_2 = 2/20/3/3/\text{balance}$ and a GHSV of 2000 h^{-1} . Temperatures are listed in the sequence as measured [for (a) and (b)].

total oxidation reactions and thereby promoting the selectivity to MAN. The results are in good agreement with the results of Heine *et al.* which propose that the active surface of the industrial VPP catalyst contains highly active V^{5+} sites separated and moderated by large quantities of phosphorus.²⁸

Two P/V_2O_5 samples were synthesized with incipient wetness impregnation with phosphorus loadings comparable the ALD sample. IWI-phosphine P/V_2O_5 and IWI-phosphate P/V_2O_5 do not show the effects observed for the ALD- P/V_2O_5 sample [see Figs. 4(c) and 4(d)]. In contrast, their character as total oxidation catalysts is even greater compared to the original V_2O_5 reference sample. Butane conversion is higher, and the selectivity to MAN even lower. No MAN at all can be detected at temperatures above 300 °C. This effect is probably not related to the presence of phosphorus, but rather to surface changes due to the interaction of the surface with the solvent during the incipient wetness impregnation. It is interesting that the phosphorus deposited via incipient wetness impregnation is not stable under reaction conditions, shown by the loss of phosphorus measured by ICP-OES. This loss can be rationalized by the fact that incipient wetness impregnation leads also to weaker bonded phosphorus species while ALD yields only chemically bound phosphorus species.

Nevertheless, the results for the sample IWI-phosphate P/V_2O_5 (multilayer) shown in Fig. 4(e) indicate that it is also possible to improve the selectivity of V_2O_5 using incipient wetness impregnation. The sample shows enhanced selectivity to MAN at low temperatures comparable to the ALD- P/V_2O_5 sample, but significantly lowers conversions of butane. The amount of phosphorus deposited via incipient wetness impregnation is high enough to cover all OH sites of the original V_2O_5 with four phosphorus atoms each. The ICP-OES results before and after catalytic testing show clearly a large loss of phosphorus, indicating that a large fraction of the phosphorus was not bound in a chemically stable way, e.g., chemisorbed on OH sites. Whether the weakly bound phosphorus atoms are distributed homogeneously over the whole surface area or form clusters on the surface can only be speculated. A comparison of the catalytic performance of ALD- P/V_2O_5 and P/V_2O_5 (multilayer) indicates that the influence of the strongly bound phosphorus species on the selectivity is similar but that less V^{5+} sites are exposed and accessible for total oxidation reactions.

IV. SUMMARY AND CONCLUSIONS

In this work, we applied V_2O_5 partially covered with phosphorus as a highly simplified model for the vanadyl pyrophosphate catalyst VPP industrially used for the selective oxidation of *n*-butane to maleic anhydride. A deposition of phosphorus using HMPT and O_3 as precursors for ALD was successful. ICP-OES, XRD, and XPS studies confirm a submonolayer of 43% of phosphorus on the V_2O_5 surface based on the total amount of available OH sites. The V_2O_5 reference sample is a total oxidation catalyst and shows no selectivity for MAN. Compared to that, the ALD- P/V_2O_5

sample shows an enhanced selectivity up to 10% for MAN in the catalytic testing and a slightly lowered activity. This result indicates that the presence of phosphorus on the surface of V_2O_5 increases the selectivity to MAN by suppressing total oxidation reactions. In addition, XRD and XPS studies indicate no formation of vanadyl pyrophosphate phase on the surface. These results agree with recent studies on the VPP surface suggesting a P-OH site located near V^{+5} as an important part of the selective site.^{13,14} In contrast, a similar loading of phosphorus impregnated on V_2O_5 via incipient wetness has no beneficial impact of the catalytic performance. An impregnation with ten times more phosphorus gives an effect similar to the deposition via ALD. However, the high concentrated impregnation sample loses around 12.5% of its phosphorus content during the catalytic testing, while the catalyst prepared via ALD is stable concerning the P content under the applied conditions. Moreover, the high P loading via impregnation does not lead to a uniform distribution of the P on the surface.

We conclude that ALD is a highly promising tool for the surface modification of catalysts, due to the strong chemical bonding of the deposited species and the uniform distribution of these species.

ACKNOWLEDGMENTS

The authors want to thank the following coworkers: S. Kohl and S. Schutte from Technische Universität Berlin. S. Lohr, M. Hashagen (BET), J. Allan and F. Girgsdies (XRD) from the Department of Inorganic Chemistry at the Fritz-Haber-Institute (FHI)/Max-Planck-Gesellschaft are acknowledged for experimental help. Special thanks to M. Bosund (Beneq Oy) for his support in Espoo. The work was conducted in the framework of the BasCat collaboration between BASF SE, the TU Berlin, and the FHI. The authors thank the Berlin Cluster of Excellence Unicat for support.

¹R. Bergman, N. J. Princeton, and N. Frisch, U.S. patent 3,293,268 (20 December 1966).

²B. K. Hodnett, *Catal. Rev.* **27**, 373 (1985).

³G. Centi, *Catal. Today* **16**, 5 (1993).

⁴G. Centi, F. Trifiro, J. R. Ebner, and V. M. Franchetti, *Chem. Rev.* **88**, 55 (1988).

⁵J.-C. Volta, *C. R. Acad. Sci. IIC* **3**, 717 (2000).

⁶G. J. Hutchings, *J. Mater. Chem.* **14**, 3385 (2004).

⁷V. V. Gulians and M. A. Carreon, *Catalysis*, edited by J. J. Spivey (RSC, Cambridge, 2005), Vol. 18, pp. 1–45.

⁸N. Ballarini, F. Cavani, C. Cortelli, S. Ligi, F. Pierelli, F. Trifirò, C. Fumagalli, G. Mazzoni, and T. Monti, *Top. Catal.* **38**, 147 (2006).

⁹E. Bordes, *Catal. Today* **16**, 27 (1993).

¹⁰P. A. Agaskar, L. de Caul, and R. K. Grasselli, *Catal. Lett.* **23**, 339 (1994).

¹¹M.-J. Cheng and W. A. Goddard, *J. Am. Chem. Soc.* **135**, 4600 (2013).

¹²M. Eichelbaum, M. Hävecker, C. Heine, A. Karpov, C.-K. Dobner, F. Rosowski, A. Trunschke, and R. Schlögl, *Angew. Chem. Int. Ed.* **51**, 6246 (2012).

¹³M. Eichelbaum *et al.*, *ChemCatChem* **5**, 2318 (2013).

¹⁴C. Heine, M. Hävecker, E. Stotz, F. Rosowski, A. Knop-Gericke, A. Trunschke, M. Eichelbaum, and R. Schlögl, *J. Phys. Chem. C* **118**, 20405 (2014).

¹⁵S. M. George, *Chem. Rev.* **110**, 111 (2010).

¹⁶V. Miikkulainen, M. Leskelä, M. Ritala, and R. L. Puurunen, *J. Appl. Phys.* **113**, 21301 (2013).

¹⁷P. C. Stair, *Top. Catal.* **55**, 93 (2012).

- ¹⁸B. J. O'Neill *et al.*, *ACS Catal.* **5**, 1804 (2015).
- ¹⁹E. Marceau, X. Carrier, M. Che, O. Clause, and C. Marcilly, *Handbook of Heterogeneous Catalysis*, edited by G. Ertl, H. Knözinger, F. Schüth, and J. Weitkamp (Wiley-VCH, Weinheim, 2008), Vol. 2, pp. 467–484.
- ²⁰K. G. Kornev and A. V. Neimark, *J. Colloid Interface Sci.* **235**, 101 (2001).
- ²¹A. A. Budneva, E. A. Paukshtis, and A. A. Davydov, *React. Kinet. Catal. Lett.* **34**, 63 (1987).
- ²²Y. V. Belokopytov, K. M. Kholyavenko, and S. V. Gerei, *J. Catal.* **60**, 1 (1979).
- ²³P. Patnaik, *Handbook of Inorganic Chemicals* (McGraw-Hill Handbooks, New York, 2003).
- ²⁴J. Hämäläinen, J. Holopainen, F. Munnik, M. Heikkilä, M. Ritala, and M. Leskelä, *J. Phys. Chem. C* **116**, 5920 (2012).
- ²⁵J. Liu, Y. Tang, B. Xiao, T.-K. Sham, R. Li, and X. Sun, *RSC Adv.* **3**, 4492 (2013).
- ²⁶J. Mendialdua, R. Casanova, and Y. Barbaux, *J. Electron. Spectrosc.* **71**, 249 (1995).
- ²⁷J. Haber, M. Witko, and R. Tokarz, *Appl. Catal. A-Gen.* **157**, 3 (1997).
- ²⁸C. Heine, F. Girgsdies, A. Trunschke, R. Schlögl, and M. Eichelbaum, *Appl. Phys. A* **112**, 289 (2013).